Improvement of Tribological Behavior of H-13 Steel by Optimizing the Cryogenic-Treatment Process Using Evolutionary Algorithms

Sanjeev Katoch[a], Rakesh Sehgal[b], Vishal Singh[c], Munish Kumar Gupta[d], Mozammel Mia[e*], Catalin Iulian Pruncu[f,g]

[a]Institute for Auto Parts & Hand Tools Technology, A-9, Phase V, Focal Point, Ludhiana-141010 (Punjab), India, email: katochsanjeev@gmail.com

[b]Department of Mechanical Engineering, National Institute of Technology, Hamirpur-177005 (HP), India, email: rakeshsehgal.nitham@gmail.com

[c]Centre for Materials Science and Engineering, National Institute of Technology, Hamirpur-177005 (HP.), India, email: vishalchib@gmail.com

[d]Key Laboratory of High Efficiency and Clean Mechanical Manufacture, School of Mechanical Engineering, Shandong University, Jingshi Road, Jinan, China, email: munishguptanit@gmail.com

[e]Mechanical and Production Engineering, Ahsanullah University of Science and Technology, Dhaka 1208, Bangladesh, email: mozammelmiaipe@gmail.com

[f]Mechanical Engineering, Imperial College London, Exhibition Rd., SW7 2AZ London, UK

[g]Mechanical Engineering, School of Engineering, University of Birmingham, B15 2TT Birmingham, UK

*Corresponding author's email: mozammelmiaipe@gmail.com

Abstract: The effect of soaking temperature and duration of cryogenic treatment cycles were investigated for the hot die steel AISI-H13 to improve its wear resistance. The amount of wear, average friction coefficient, and maximum local contact temperature were investigated against the AISI D3 cold work tool steel (hardened and tempered) used as counter-surface for five conditions – varying the loading and sliding speed. Sliding parameter has great influence over wear rate when is compared to load effects. The wear detected on the surface analyzed is adhesive wear produced by deformation lips, surface cracks and fractured ridges. To achieve an increase of efficiency, Particle Swarm Optimization is preferred as it showed lower deviation than Bacteria Foraging Optimization in optimized results.

Keywords: Cryogenic treatment; Coefficients of friction; Wear amount; Intelligent optimization.

Nomenclature

A3T : Hardening at = 1040 °C, for 30 Minute followed by Nitrogen gas quench at quench pressure of 5 bar. No cryogenic treatment. Three tempering at 550 °C, 570 °C, 620 °C respectively for 2 hours

BFO : Bacterial foraging optimization

CT : Cryogenic treatment

C1 : Cryogenic Treatment at -154°C

C2 : Cryogenic Treatment at -184°C

PSO : Particle swarm optimization

RSM : Response surface methodology

ST : Soak time

R_a : Surface roughness

T_M : Maximum local contact temperature

W_R : Wear Rate (gm/m)

μ_0 : Average friction coefficient

1. Introduction

Different techniques are prevailing in the industry since long for the enhancement of tribological behavior of tools through the modification of surface chemical composition and morphology of its microstructure. Widely and commonly employed methods for the structural and engineering steel to modify its surface's physical and mechanical properties are nitriding and carburizing. In case of tool and die steel physical / chemical vapor deposition and plasma nitriding methods are utilized for the enhancement of surface properties for corrosion and wear resistance [1-3]. The employment of above-mentioned techniques only alters the surface metallurgy/chemical composition of material – thus only improves the surface characteristics linked to the hardness, amount of wear, fatigue resistance, corrosion and/or coefficients of friction of the post processed materials (e.g. heat treated).

Normally, these surface modification processes use toxic chemicals which affect the environmental quality, health issues, energy consumption and therefore are not environmentally friendly. The cryogenic treatment (CT) is one of the latest environmentally friendly material treatment processes with a fast growth rate since last couples of decades. It generates the material quality improvement at atomic level with cost reduction and optimum

productivity. The cryogenic treatment is produced at very cold condition using particular fluids (i.e. liquid nitrogen, helium and/or hydrogen). The boiling state of a given processing media lies below -154ºC [4]. Therefore, this treatment is close to these fluids limit saturation (e.g. liquid nitrogen having a boiling point of -196ºC). These fluids are considered colorless, having no odor, or no taste and almost non-toxic gases, which put this method in the category of clean and environmentally friendly processes.

CT is a dry process and emerges as an environmentally friendly method. In this process, the liquid nitrogen, transformed in a gas, is introduced in a chamber in which the treatment occurs with better quality for tool/work-piece interface. It permits to reduce the harsh contact between the tool/workpiece and further allows eliminating the cracking potential during rapid cooling on the treatment cycle. Therefore, the CT is leading to better process for the tool having extended life and suitable mechanical properties during working condition [5, 6].

In the recent past, most researchers demonstrated that CT plays a key role in morphology improvements for cold and hot work tool steel microstructure and hardness [7-19]. Effect of different holding time at CT has been studied by the Amini et al. [12] when tribological behavior assessment was simulated varying parameters like load and/ speed of sliding. They found that holding time of 48 hours at cryogenic temperature is optimal for the wear resistance maximization of 80CrMo12 5 steel. By varying the CT was possible to reduce the wear amount for tool steel material produced by cold working. It was investigated by Das et al. [8] and concluded that for this grade of steel 36 hours is optimal holding time to accomplish maximum wear resistance. Cryogenically treated bearing steel grade AISI 52100 for holding time 12, 24, 36, 48 and 60 hours at temperature -145°C was investigated by Gunes et al. [13] using ball- disk arrangement. They also found that for this grade of bearing steel 36 hours as the optimal soaking time. The improvements in Tungsten Carbide tools dedicated for turning process was developed by treatments like deep cryogenic by Yong et al. [15]. Using the later process is possible to enhance the wear resistance in terms of chipping when cutting in continuous mode is imposed for limited periods of time. Drill High speed tool steel grade M2 for drilling operation of normalized medium carbon steel grade CK 40 was studied by Firouzdor et al. [14] and they claimed that deep CT enhances the resistance to wear for grade M2 steel when is compared with untreated one. Therefore, CT can act as potential facilitator for generating the fine carbide precipitation when the martensite becomes super saturated.

The CT features for martensitic transformation of the specific X153CrMoV12 steel at temperature below −100 °C was investigated by Gavriljuk et al. [17]. They concluded that at low-temperature martensitic transformation occurred owing to plastic transformation and subsequent tempering results in the precipitations of carbides and affects the properties X153CrMoV12 steel. Mechanical properties and carbides precipitation from the matrix of cryogenically treated tool steel augmented with the post tempering [18]. The CT has the potential to improve the tool made of steel used for tribological work whereas the fracture toughness is also dependent on its chemical composition and type of treatment given to it [19].

The state of art proves the great potential of using CT that effectively produces improvements to the mechanical and tribological features especially for tools (dies from steel). However, the full benefits in terms of productivity and cost effectiveness are limited because this process occur in critical condition and is difficult to maneuver it. An optimization routine may demonstrate its power when the CT process is validated on specific tools (e.g. dies) made of diverse grade of steel.

An optimum CT is a crucial objective to further increase the accuracy and reduce the cost. Some classical optimization models (e.g. Taguchi strategy, the RSM and regression algorithms) were proposed with success in order to better control the wear amount on the materials treated at cryogenic temperatures [20-22]. However, these traditional methods are less accurate and very weak because they produce only a local solution. Recently, other evolutionary strategies (i.e. PSO, Genetic Algorithm (GA), Artificially Bee Colony (ABC) and BFO etc.) gained popularity due more consistency [23]. Though, each of them indicates some inconvenience when manufacturing process was simulated. The PSO and BFO proved promising evidence (i.e. less resources and high accuracy) when different manufacturing routines were optimized [23-27]. From our research, there is no study regarding the optimization through PSO and BFO for the cryogenically treated HDS AISI H13 that allows to improve the friction and wear resistance. This research attempts to explore the benefits of optimization algorithms (i.e., PSO and BFO) to the CT process parameters in terms of tribological behavior (i.e. wear resistance, the average friction coefficient, and maximum contact temperature). The validation was performed simulating the AISI H13 steel in dry sliding contact with a hardened and tempered cold work tool made of AISI D3 steel as counter face.

2. Materials and methods

In the experiments were selected the material made of AISI-H13. Its chemical composition was measured using the ASTM E 415-2014 [28] guidance with a spark emission spectrometer and contain following elements: 0.40-C; 0.86-Si; 0.36-Mn; 5.05-Cr; 1.30-Mo; 0.98-V; 0.018-P; 0.007-S; balance –Fe in wt% [1].

A hardened (52 HRc) cold work tool steel AISI D3 (containing in wt%: 2.02-C; 0.18-Si; 0.40-Mn; 12.60-Cr; 0.10-V; 0.021-P; 0.026-S; balance –Fe [12]) roller of outer diameter 60mm, inner diameter 25mm, and thickness 20mm was used as the counter face material.

The wear testing sample blocks of 6.35x6.35x9mm were machined from round steel bar using Wire Electrical Discharge Machine accordingly to the ASTM G 77-05 RA 2010 [29]. To perform the assessment of varied CT effect on surface morphology of AISI H-13. In conformity with ASTM E3-01 RA 2007 [30] some samples were cold mold in resin followed by grinding, and polishing by silicon carbide sand paper. Polished Specimen were etched using a solution containing 97% Nitric Acid + 3% Ethanol followed by hot air drying. The surface morphology was analyzed by a Field Emission-Scanning Electron Microscope (FE-SEM) mark: Quanta FEG450 make: FEI, Holland.

The hardness was evaluated under a Micro Vicker hardness tester, model: MVK-H2, make: Akashi, Japan, by following ASTM E384-08 [31]. During the indentation was used a testing load of 1000gf (9.8N) for 15 second. To get the average and uniform apparent hardness load of 1000gf (9.8N) was chosen so that localized hardness of single phase can be avoided (i.e., carbide or austenite or martensite). For repeatability, an average of five hardness readings for each sample was measured.

2.1 Sample Treatments

Hardening of samples was performed in the vacuum heat treatment furnace keeping a constant temperature of 1040° C during 30 minute holding time; later on, the sample was submitted to nitrogen gas quenching and then sample was subjected to one tempering for 2 hours holding time at 550° C. After this, the samples were divided in to seven categories and different types of treatment were given to the samples. Figure 1 shows the heat treatment and cryogenic treatment cycle given to the samples under study. Table 1 shows the details of samples treatment and their respective code.

2.2 Experimental procedure

The full factorial design approach was developed to create the experimeantal work on conventionally and varied cryogenically treatment samples. It was generated on Design–Expert 7.1 (Stat-Ease, USA) software. By using this technique (i.e. full factorial design) it is possible to identify an individual effect derivate from the variable response and interaction activity [32]. In Table 2 are introduced all the parameters that allow to estimate the wear effect.

The wear resistance was simulated on treated and hexane cleaned block (6.35 x 6.35 x 9mm) samples using a Multi Tribo tester. The experiments were designed as per ASTM G77-05 [29]. The total number of matrix experiments was 175. To produce a new sample free of defect with a surface roughness (R_a) <0.2µm the counter face roller was grinded by SiC paper up to 1000. The local temperature of the contacting surface was measured with a non-contact type infrared thermometer having resolution: 0.2°C and accuracy level of ±2.5% or 2.5 °C. An electronic precision analytical balance was used to weigh the samples before and after each experiment with an accuracy of 0.00001gm that permits to estimate the wear rate.

2.3 Particle Swarm Optimization (PSO)

This technique is considered as a stochastic one and generated the optimization process by following a biological structure (which reproduce the fish schooling and/or bird flocking). It contains some generalities from GA, however does not consider the classical genetic operator that is based on crossover and mutation. The PSO deals with an internal velocity and a proper memory generating better autonomy for algorithm update during processing. Moreover, the PSO enabling massive potential as it includes specific characteristics from evolution strategies (ES) and/or generic algorithms (GA) [33].

During the PSO process, the algorithms reproduce the bird's movements as a group from natural environment. Considering a simple vector is possible to reproduce the swarm and movement of each individual bird that form the bird flocking (that ascribe the intelligent agents or particles used in PSO). Though, the intelligent agents or particles allow producing different numbers of iterations that are determined randomly. They generate update with the last positions when certain velocity is reached according to pbest i.e., which represent the best search location for a specific particle and gbest i.e., which represent the best particle location

from the entire population. The pbest location is automatically replaced by the gbest location, if in the algorithm during iteration the intelligent agents or particles best position overcome the global best [24-26].

2.4 Bacterial Foraging Optimization (BFO)

The BFO strategy imitates the process produced by the biological motile bacteria (i.e. E. Coli and Salmonella) developed in the food product. Usually, these bacteria are guided by the aid of locomotive flagella when produce the search in space from which they pick up the nutrients and avoid noxious substances. They movements occurs in the clockwise or anticlockwise rotation of the flagella when search to locate the best nutrient either moving in a systematic manner (swim or run) or tumble chaotically. Further, their movements are derived by the nutrient concentration for the search activity in space. It was demonstrated their generality to swim more than tumble in a random direction once the nutrient is more concentrated. Chemotaxis is the term that ascribe the tumble or swim movement pattern of bacteria for foraging of nutrient food [27, 33].

3. Results and discussion

3.1 *Evaluation of responses during dry sliding conditions*

The experimental responses aquired as wear rate (W_R), average friction co-efficient (μ_o) and maximum local contact temperature (T_M) during the dry contacting conditions are shown in Table 3. To reduce the variability in the process, it is indicated to obtain a variance stabilization produced by a transformation [34]. Hence, for building up the mathematical model, the normality of data and homogeneity of variance were taken into the central thought. Transformation is always helpful to keep stable the variance. The stability of variance improves the process normality. Therefore, Box-Cox technique was implemented (using software Design–Expert 7.1) on the experiments responses to have power transformation.

The acquired Box-Cox plot (Fig.2) by implementing above mentioned technique is in the range of $\pm$ 3 σ. In Fig.2 the point where green line intersected the curve (U-shape) is the best transformation (i.e., λ=0). On the U-shape curve of Box-Cox plot the best transformation with 95% confidence level for the upper and lower limit shown by the small pink lines intersection

(Fig. 2). In the case of "W_R", the best transformation limits (the upper and lower limit) was identified between $-0.03 < \lambda < 0.03$. Therefore, there is not any $\lambda = 1$, and shows that transformation will be beneficial. For best fitting of the model, the greatest approximation occurs when "λ" reduces its error to a sum up of a squares [35]. For a suitable fitting (finest fitting) is worth to obtain a determined log transformation ($\lambda = 0$). In Fig.2, a point that is obtained by the intersection of a vertical short blue line with the U-shape curve represents the potential of a best-recommended conversion (at $\lambda = 0.0$) generated by the software for the "W_R". The same steps has been done for the rest of the responses (i.e. "μ_0" and T_M), which conforms for the transformation of the experimental response data. To confirm the normal distribution of residuals, the internal studentized residual versus normal percentage probability curve is plotted (Fig.3).

Except of few data points, identified at lower and upper portion of central line all other data point nearer to it. This indicates the normal distribution of residuals. In Fig.4 were plotted the obtained data described by the $\pm 3\sigma$ range in order to sort out the discrepant data residuals versus run plot. As the points are located inside of the range it demonstrates that the model is fitted very well with 95% confidence level. Predicted value of responses versus actual responses plot (Fig.5) examined to find out outlier data. Figure 5 shows that all data points are placed nearer to the central reference line (at 45° position). This indicates and endorses the model as suitable to describe the wear evolution considering its parameters.

This model selected for investigation was based upon the "R^2" values. The "R^2" close to 1, represents that data fits the well in a regression line [36]. Cubic model recommended by the analysis for the "W_R" with adjusted "R^2"= 0.9986, predicted "R^2"= 0.9981 at p-value < 0.0001. ANOVA is tailored manually by removing the all insignificant terms. The same steps have been performed for the rest of the responses (i.e. average friction co-efficient and the maximum local contact temperature). The coefficient of determination values using response parameters data are shown in Table 4.

3.2 Effect of cryogenic treatment parameters for the tribological performances

Wear rate (W_R): This was detected (see Table 3) in Figure 6 for specific selection of operating normal load (60-140N) and speed of sliding (between 0.628 - 1.886 m/s). When low speed of sliding was imposed (i.e. 0.628 m/s to 1.257 m/s) the "W_R" is more noticeable. In the mid-range of sliding speed (e.g. 1.257 m/s or 1.571 m/s) a sharp increase in the "W_R" was

observed. Further, when a relatively higher speed of sliding was imposed (e.g. 1.885 m/s) it promotes a decreasing trend of "W_R" for these CT samples.

The cryogenic-processed specimens demonstrated (see results from table 5 compared with Table 3) that the "W_R" have a low progress in respect to a sample without cryogenic treatment either of loading conditions and speed of sliding. Lower "W_R" was evidenced up to holding time of 21 hours in cryogenically treated samples. However, a holding time of 36 hours increases the "W_R". A similar trend was observed by Amini et al. [12] for investigation of tool made of steel (i.e. 80CrMo12 5); Das et al. [7] detected this behavior for D2 tools; others like Gunes et al. [13] observed it on AISI 52100 bearing components. As the holding time increases there is reduction in the hardness value which causes the reduction in wear resistance. It agrees with the findings of [12] that associate the best wear resistance for the CWS 80CrMo12 5 occurred when CT was hold for 48hrs. Generations of optimum "W_R" for AISI D2 CWS is produced when the holding time during CT is 36 hrs stressed by Das et al. [7]. Additionally, Gunes et al. [13] detected the best "W_R" for AISI 52100 when the holding time during CT is 36hrs.

The study of worn surface revealed the adhesive wear, deformation lips, surface cracks and fractured ridges (Fig. 7). Metalic-plate type wear debris was found and it varied with the type of treatment operating set of wear experiment parameters (i.e. applied normal load and sliding velocity). In case of A3T treated samples the wear debris size is more comparable to cryogenically treated samples. C2-36 sample has the deformation lips, fractured ridges and sub-surfaced cracks and adehsive wear. C2-36 reveals a low hardness value that leads to accentuated plastic behavior. The particles accumulated in the surface indicates the activation of lumps of wear formed formed as initial adhesive wear process [37].

Average friction co-efficient (μ_o): The normal load applied and the speed of sliding is directly proportionally with "μ_o" magnitude. Therefore, it was observed from Figure 8 that the higher friction value for a bigger load value combined with a faster speed of sliding. Fluctuation in the "μ_o" at normal load and sliding velocity might be owing to low value of surface contact stress = 1.48 MPa as compared to higher load = 3.47 MPa. The samples submitted to CT shows a lower "μ_o" when are compared to untreated samples A3T when is varied the operating settings to simulate the wear process. The cryogenically treated specimens were responsible for having a higher amount of non-dissolved carbon in the martensitic matrix; therefore leading to

an increased hardness and elastic limit in comparison with the conventionally treated ones. They are responsible for decreasing the friction and acts only marginally to decrease the wear coefficient [38].

Maximum contact temperature (T_M): The "T_M" of tribo-pair increased with increasing value of sliding speed and load, as exhibits in Figure 9. At all levels of selected applied normal load in the range of 60-140N combined with the sliding velocity that vary from 0.628m/s to1.885m/s the "T_M" of tribo-pair raises from 21.6 to 93.0°C. This was noted for all cases of tested samples in the experiment. "W_R" decreases with the rise in temperature. It might be due the transfer of heat to a moving mass parts [39].

Hardness: Figure 10 shows the measured micro hardness values (HV_1) for treated samples. There was detected almost 3.1% enhancement in the C1-6 treated sample when is compared to samples H3T treated that proves to be superior when associated to other cryogenically treated samples. It is because the cryogenic treatment can eliminate retained austenite, allows to generate a better carbide distribution, and further increases the carbide content [40]. The samples denoted as C1-6 and C2-6 and obtained following a treatment with 6 hrs holding time indicates in their surface higher micro-asperities. When C2- is treated with 36 hrs holding time was observed a decrease into the micro-asperities in respect to the H3T ones. The decrease was approx. 4% for the C1 – 36 and a decrease of 5.2% for the C2-36. The observation agrees well with the findings of Das et al. [8]. By applying the same strategy Amini et al., [12] detected a lower hardness when investigated tool made as cold work from steel 80CrMo12 5. The higher cryogenic soaking times generate significant improvements in hardness and wear resistance [41].

Surface morphology: The as received samples AISI-H13 steel were investigated for their morphology (see details Figure 11a). There, the ferrite matrix contains some globular carbides. Fig. 11b shows a A3T treated sample and shows laths of martensite, fine globular carbide alongwith retained austenite. Figure 11c–h presents FESEM micrograph of cryogenically processed samples C1-6, C1-21, C1-36, C2-6, C2-21 and C2-36 respectively. The cryogenically processed samples indicate the occurrence of precipitated secondary phase of carbide distributed evenly and very dense in respect to samples of A3T. They receive the effect of deep cryogenic treatment that is produced in the acceleration on the Ostwald ripening

process [41]. It is suspected that the CT permits to increase the driving force for the nucleation of carbides and the number of carbides increased while the carbides size was decreased [42]. Besides, the patterns of lath martensite in coarse geometry were detected when longer holding processing time was used. Fig. 11c-h highlights a decrease on austenite phase that was replaced by the martensite phase. Therefore, it seems that the micro structure changes related to CT helps to generate an austenite reduction and carbide precipitation. It leads to produce improvements over material resistance by an increase its hardness [43] and [44]. The agglomeration of fine carbide particles can further lead to other materials features (i.e. strength, toughness or wear resistance) [8, 13].

CT enhanced the tough tempered martensite phase and reduced the retained austenite; thus, improved the toughness and strength of matrix [8,13,16,18]. On the other hand, it is believed that CT removes retained austenite [9,16,45], the complete or near to complete transformation of retained austenite into martensite [14, 8], precipitation of η-carbides [46], fine carbides formation with regimented distribution of carbides [12], decay of martensite leading to boosted precipitation of distinguished secondary carbides with more consistent dispersal [14,11,47]. As the fractional disbanding of brittle primary carbides is supposed to be accountable for the toughness since the decrease in soft retained austenite content [45]. Hence, with the appropriate selection of CT process parameters concurrent improvement of hardness and toughness can be achieved as demonstrated in the case of tool steel 45WCrV7 by Vahdat et al. [48].

3.1 Optimization using desirability, PSO and BFO method

By developing a careful optimization strategy that incorporates the desirability function and was applied through PSO and BFO detected the best parameters for input (i.e., holding time at cryogenic temperature for the cryogenic treatment cycle for low value of "W_R", "μ_s" and "T_M"). Three different responses were evaluated by polynomial equations. The wear rate and local contact temperature are represented by a normal log whereas the friction evolution was determined as linear one. From there, it was produced specific plot in which the best factor was sorted for each variable. In this strategy, the best condition is achieved once the numerical value of each variable is close to the maximum of total desirability function.

Desirability function method: Table 5 offers a summary of results obtained from optimization strategy (developed using the desirability function) leading to improve the tribological parameters. There were used 7 different levels of combination termed as categorical factor. To check the features of simulations developed by mathematical algorithms the specific conformity tests were embedded. It permits to endorse the viability of models formulated as per experiments determination. Taking into account the results as an average determined by experiment confirmation and confronted to the predicted one, were noted a very good agreement between their responses (see details on Table 6). We can highlight the robustness of the model with a very small variance that is only 2-9%.

PSO: The main parameters used in this formulation were inserted in Table 7. Further, Table 8 presents a summary of results optimized through PSO strategy and the details of experimental data values were inserted for confrontation. The results matched very well (predicted vs the experimental values). Some small variations were achieved that is only 5-11%. The robustness of the model is recognized by the high success rate which is around 90% and requires very limited time of processing that is 1.02 seconds.

BFO: It was proposed firstly by Passino [27]. The main parameters used in this formulation were inserted in Table 9. Further, Table 10 presents a summary of results optimized through BFO strategy and details of experimental data values was inserted for confrontation. The results match very well (predicted versus the experimental values). Some small variations were achieved that is only 5-19%. Yet, this method seems very robust but weaker than PSO. The success performances reach only 80% and require longer time of processing that is 10.23 seconds. Pbest and Gbest mechanisms permit a higher productivity for the PSO strategy while the complexity of BFO denoted by large numbers of computation steps make the later one weaker in respect to PSO. Fig. 12 presents details of PSO and BFO structure.

Cryogenic treatment is reported as one of the methods useful for improving the properties of the materials. But, because of complexity of the process in implementation, change in mechanisms for different materials is still unpredictable. Further investigation would be required to make it possible for implementation as in case of conventional heat treatment

process. The critical parameters of the process like cooling rate, soaking temperature, soaking duration, warming rate and tempering cycles are required to be investigated depending on the various materials and optimum properties needed in these cases. The study can be extended in the form of modelling and simulation of the process.

4. Conclusions

In this study, the parametric evolutionary optimization techniques have been applied to find out the optimal conditions that enable to minimize the wear rate (W_R) and the average friction coefficients (μ_o) when they are corroborated with the maximum local contact temperature (T_M). This strategy of optimization permits to increase the efficiency of cryogenic treatment applied to HDS H13 material used in manufacturing for tooling applications (i.e. forming) which act as counterpart within the dry sliding process. In the proposed tribological trials, the counter subject material selected was a cold work steel (i.e. AISI D3). The simulation of dry sliding was performed using specific operation settings (by varying the normal load between 60-140N and speed of sliding between 0.628-1.885m/s, respectively). The results can be summarized as follows:

- The speed of sliding parameter was found to have a great influence over "W_R" when is compared to load effects. It was detected that the holding time of 21 hours during the cryogenic treatment temperature is the optimal setting in order to obtain the lowest "W_R" (Treatment: C2-21).
- The applied normal load (in the range of 60-140N) combined with the sliding velocity (varied from 0.628m/s to1.885m/s) produces an increase of the maximum contact temperature that raises from 21.6 to 93.0°C. However, it was noted that the "W_R" decreases with the rise in temperature.
- The main wear detected on the surface analyzed is adhesive wear produced by deformation lips, surface cracks and fractured ridges (i.e. metallic debris).
- The samples treated by CT demonstrated lower "μ_0" in respect to untreated samples A3T when was varied the operating settings to simulate the wear process. This is because, the cryogenically treated specimens possess superior hardness values acquired during the treatment.

- The deviation among the desirability approach from the predicted results and experimental one is in the range of 8.7%, 3.2% and 7.4% for "W_R", "μ_o" and "T_M", respectively, and the best solution were identified in the optimized treatment of type (i.e., C2-21).
- The deviation among the PSO predicted results and experimental ones are in the order of 2%, 11% and 1% for "W_R", "μ_o" and "T_M" respectively for the predicted optimized treatment type (i.e., C2-21).
- The deviation among the BFO predicted results and experimental are in the order of 5%, 19% and 4% for "W_R", "μ_0" and "T_M" respectively for the predicted optimized treatment type (i.e., C2-21).

Finally, the adaptation of intelligent evolutionary algorithms in the domains of critical engineering such as wear and tribology opens the possibility of sophisticated advanced optimum results that is hardly achievable by implementing traditional statistical methods.

References

[1] Holmberg K, Matthews A. Coating tribology: properties, techniques, and applications in surface engineering: Elsevier; 1994.

[2] Leite M, Figueroa C, Gallo SC, Rovani A, Basso R, Mei P, et al. Wear mechanisms and microstructure of pulsed plasma nitrided AISI H13 tool steel. Wear. 2010;269:466-72.

[3] Wang J, Xiong J, Peng Q, Fan H, Wang Y, Li G, et al. Effects of DC plasma nitriding parameters on microstructure and properties of 304L stainless steel. Materials Characterization. 2009;60:197-203.

[4] Diekman F, Papp R. Cold Facts about Cryogenic Processing. Heat Treating Progress. 2009;9:33-6.

[5] Lal DM, Renganarayanan S, Kalanidhi A. Cryogenic treatment to augment wear resistance of tool and die steels. Cryogenics. 2001;41:149-55.

[6] Barron R. Effect of cryogenic treatment on lathe tool wear. Proceedings of the 13th International Congress of Refrigeration1973. p. 529-34.

[7] Das D, Dutta AK, Ray KK. Sub-zero treatments of AISI D2 steel: Part I. Microstructure and hardness. Materials Science and Engineering: A. 2010;527:2182-93.

[8] Das D, Dutta A, Ray K. Influence of varied cryotreatment on the wear behavior of AISI D2 steel. Wear. 2009;266:297-309.

[9] El Mehtedi M, Ricci P, Drudi L, El Mohtadi S, Cabibbo M, Spigarelli S. Analysis of the effect of deep cryogenic treatment on the hardness and microstructure of X30 CrMoN 15 1 steel. Materials & design. 2012;33:136-44.

[10] Koneshlou M, Asl KM, Khomamizadeh F. Effect of cryogenic treatment on microstructure, mechanical and wear behaviors of AISI H13 hot work tool steel. Cryogenics. 2011;51:55-61.

[11] Katoch S, Sehgal R, Singh V. Evolution of mechanical properties and microstructure of differently cryogenically treated hot die steel AISI-H13. Int. J. Mater. Res.2017; 108(3): 173. DOI: 10.3139/146.111467.
[12] Amini K, Nategh S, Shafyei A. Influence of different cryotreatments on tribological behavior of 80CrMo12 5 cold work tool steel. Materials & design. 2010;31:4666-75.
[13] Gunes I, Cicek A, Aslantas K, Kara F. Effect of deep cryogenic treatment on wear resistance of AISI 52100 bearing steel. Transactions of the Indian Institute of Metals. 2014;67:909-17.
[14] Firouzdor V, Nejati E, Khomamizadeh F. Effect of deep cryogenic treatment on wear resistance and tool life of M2 HSS drill. Journal of Materials Processing Technology. 2008;206:467-72.
[15] Yong A, Seah K, Rahman M. Performance of cryogenically treated tungsten carbide tools in milling operations. The International Journal of Advanced Manufacturing Technology. 2007;32:638-43.
[16] Huang J, Zhu Y, Liao X, Beyerlein I, Bourke M, Mitchell T. Microstructure of cryogenic treated M2 tool steel. Materials Science and Engineering: A. 2003;339:241-4.
[17] Gavriljuk V, Theisen W, Sirosh V, Polshin E, Kortmann A, Mogilny G, et al. Low-temperature martensitic transformation in tool steels in relation to their deep cryogenic treatment. Acta Materialia. 2013;61:1705-15.
[18] Li S, Wu X. Microstructural evolution and corresponding property changes after deep cryotreatment of tool steel. Materials Science and Technology. 2015;31:1867-78.
[19] Podgornik B, Paulin I, Zajec B, Jacobson S, Leskovšek V. Deep cryogenic treatment of tool steels. Journal of Materials Processing Technology. 2016;229:398-406.
[20] Darwin J, Lal DM, Nagarajan G. Optimization of cryogenic treatment to maximize the wear resistance of 18% Cr martensitic stainless steel by Taguchi method. Journal of Materials Processing Technology. 2008;195:241-7.
[21] Darwin J, Mohan Lal D, Nagarajan G. Optimization of cryogenic treatment to maximize the wear resistance of Chrome Silicon spring steel by Taguchi method. Int J Mat Sci. 2007;2:17-28.
[22] Senthilkumar D, Rajendran I. Optimization of deep cryogenic treatment to reduce wear loss of 4140 steel. Materials and Manufacturing Processes. 2012;27:567-72.
[23] Gupta M, Singh G, Sood P. Modelling and optimization of tool wear in machining of EN24 steel using taguchi approach. Journal of the Institution of Engineers (India): Series C. 2015;96:269-77.
[24] Kennedy J. Particle swarm optimization. Encyclopedia of machine learning: Springer; 2011. p. 760-6.
[25] Gupta MK, Sood P, Sharma VS. Machining parameters optimization of titanium alloy using response surface methodology and particle swarm optimization under minimum-quantity lubrication environment. Materials and Manufacturing Processes. 2016;31:1671-82.
[26] Gupta MK, Sood P, Sharma VS. Optimization of machining parameters and cutting fluids during nano-fluid based minimum quantity lubrication turning of titanium alloy by using evolutionary techniques. Journal of Cleaner Production. 2016;135:1276-88.
[27] Passino KM. Biomimicry of bacterial foraging for distributed optimization and control. IEEE control systems. 2002;22:52-67.
[28] ASTM E. E 415-2014. Standard test method for Analysis of carbon and low alloy steel by spark atomic emission spectrometry. ASTM Annual Book of Standards. 2014.
[29] G77-05 A. Standard test method for ranking resistance of materials to sliding wear using block-on-ring wear test. 2010.

[30] ASTM. Standard guide for preparation of metallographic specimens. 2011.
[31] Standard A. Standard Test Method for Microindentation Hardness of Materials. 2002.
[32] Mia M, Dhar NR. Prediction and optimization by using SVR, RSM and GA in hard turning of tempered AISI 1060 steel under effective cooling condition. Neural Computing and Applications. 2017.
[33] Mukherjee I, Ray PK. A review of optimization techniques in metal cutting processes. Computers & Industrial Engineering. 2006;50:15-34.
[34] Montgomery DC. Design and analysis of experiments: John Wiley & Sons; 2008.
[35] Katoch S, Sehgal R, Singh V. Optimization of friction and wear characteristics of varied cryogenically treated hot die steel grade AISI-H13 under dry condition. Friction. 2017;5:66-86.
[36] Mia M. Mathematical modeling and optimization of MQL assisted end milling characteristics based on RSM and Taguchi method. Measurement. 2018;121:249-60.
[37] Lohith KM, Sondur V, Sondur V. The Effect of Cryogenic Treatment on the Hardness, Friction and Wear Resistance of Austenitic Ductile Iron Type D3 Tool Steel. Journal of Modern Engineering Research. 2014;4:24-9.
[38] Prieto G, Bakoglidis KD, Tuckart WR, Broitman E. Nanotribological behavior of deep cryogenically treated martensitic stainless steel. Beilstein journal of nanotechnology. 2017;8:1760.
[39] Sharma M, Sehgal R, Pant M. Tribological behavior of Ti3Al2. 5V alloy sliding against EN-31 steel under dry condition. Tribology transactions. 2016;59:451-61.
[40] Amini K, Akhbarizadeh A, Javadpour S. Effect of deep cryogenic treatment on the formation of nano-sized carbides and the wear behavior of D2 tool steel. International Journal of Minerals, Metallurgy, and Materials. 2012;19:795-9.
[41] Yao Y, Zhou Y. Effects of Deep Cryogenic Treatment on Wear Resistance and Structure of GB 35CrMoV Steel. Metals. 2018;8:502.
[42] Rhyim YM, Han SH, Na YS, Lee JH. Effect of Deep Cryogenic Treatment on Carbide Precipitation and Mechanical Properties of Tool Steel. Solid State Phenomena. 2006;118:9-14.
[43] Manjunatha L, Lokesha M, Ajaykumar B. A review: Mechanical Properties of HSS Steel by deep Cryo-Treatment. IOP Conference Series: Materials Science and Engineering: IOP Publishing; 2018. p. 012098.
[44] Idayan A, Gnanavelbabu A, Rajkumar K. Influence of Deep Cryogenic Treatment on the Mechanical Properties of AISI 440C Bearing Steel. Procedia Engineering. 2014;97:1683-91.
[45]Nanesa NG, Jahazi M. Simultaneous enhancement of strength and ductility in cryogenically treated AISI D2 tool steel. Mater. Sci.Eng. A. 2014; 598: 413.
[46]Meng F, Tagashira K, Azuma R, Sohma H. 1994) Role of η - Carbide precipitation in the wear resistance improvement of Fe-12Cr-Mo- V-1.4C tool steel by the cryogenic treatment. ISI Journal International. 1994; 34(2):205.
[47]Ray K K, Das D. Improved wear resistance of steel by cryotreatment: the current state of understanding', *Mater. Sci. Technol.* 2016; doi: 10.1080/02670836.2016.1206292.
[48] Vahdat SE, Nategh S, Mirdamadi S. Microstructure and tensile properties of 45WCrV7 tool steel after deep cryogenic treatment. *Mater. Sci. Eng. A*, 2013;585: 444.

Figure(s)

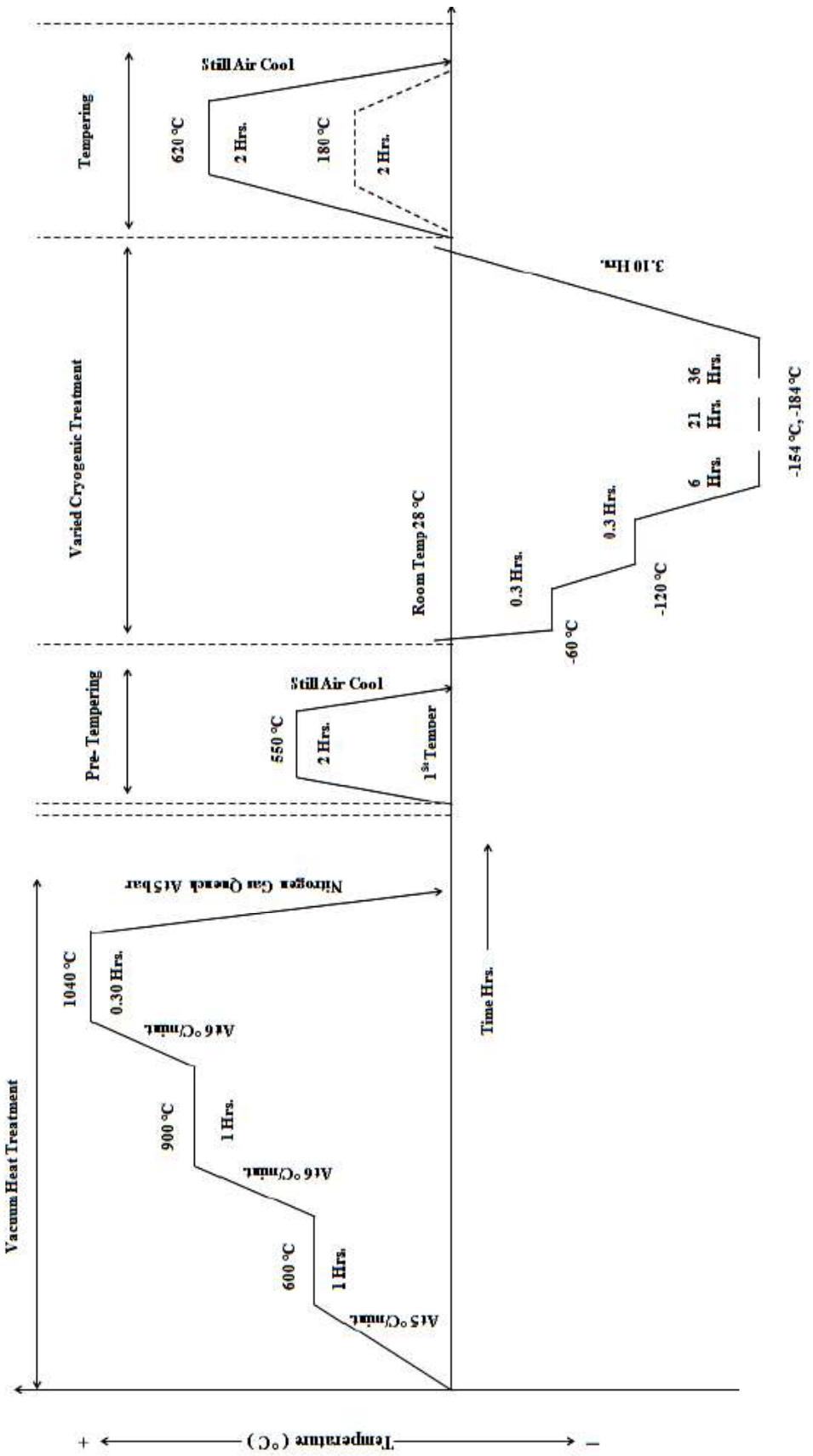

Fig.1. Samples treatment cycle schematic

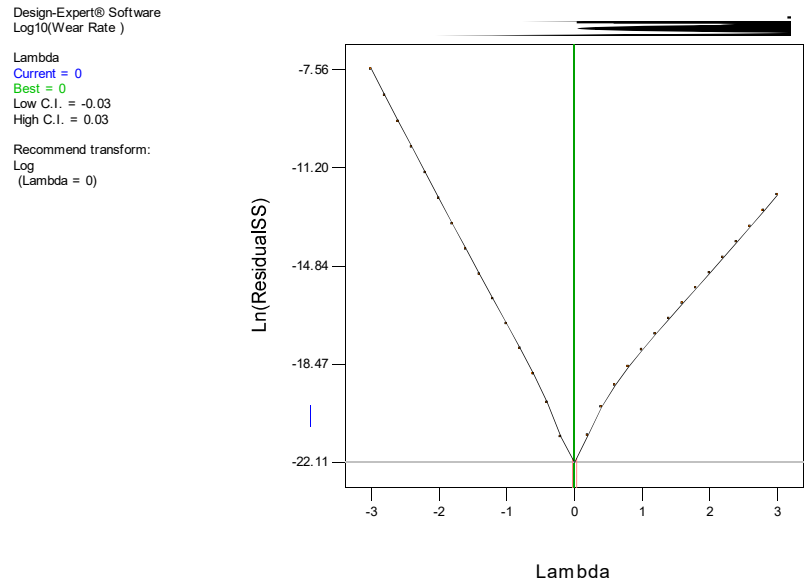

Fig.2. Power transformation Box-Cox plot for "W_R"

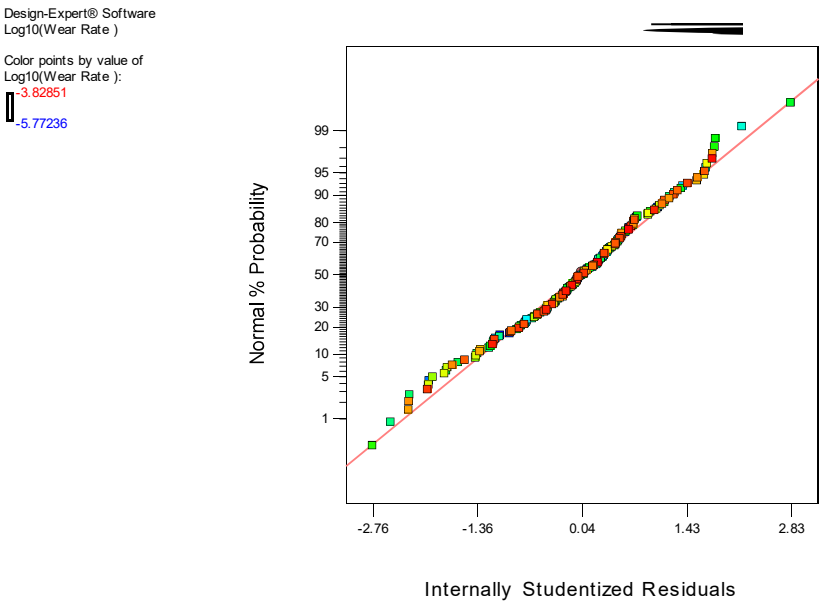

Fig.3. Plot of residuals for "W_R"

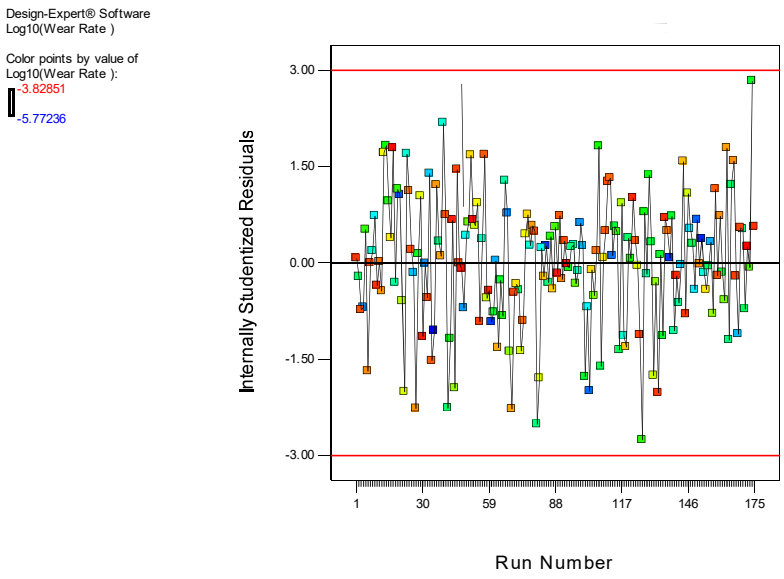

Fig.4. Experimentation runs order for "W_R"

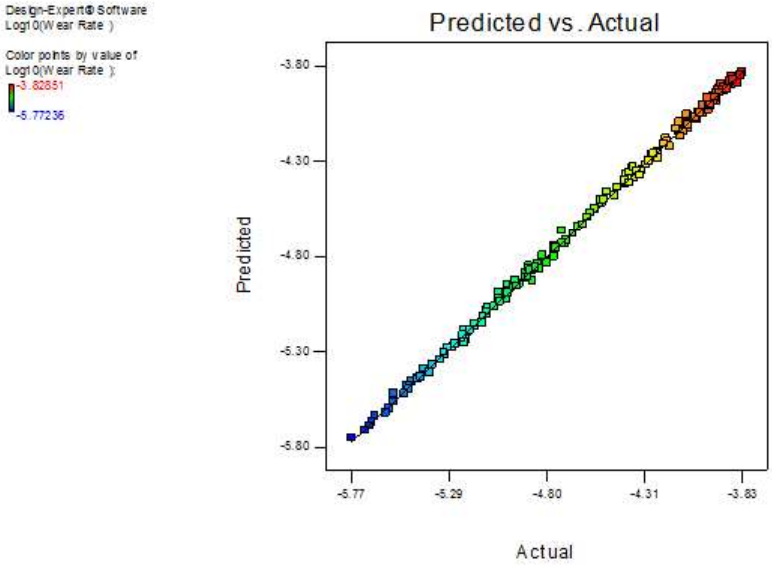

Fig.5. Predicted versus actual value for "W_R"

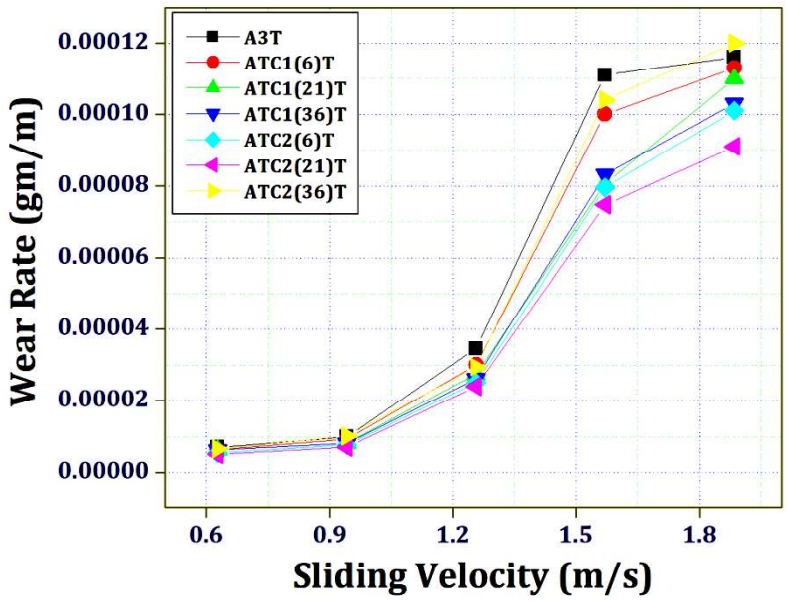

(a)

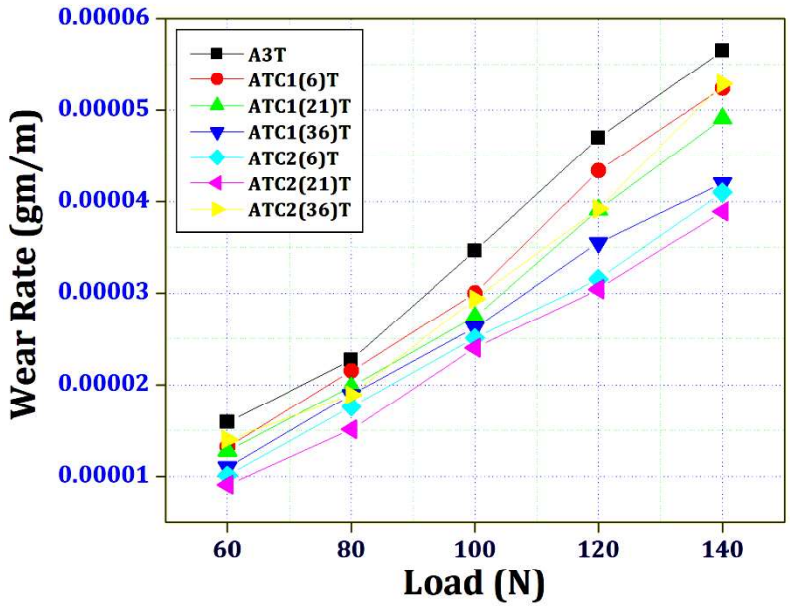

(b)

Fig. 6. Effect of process parameters on wear rate (a) Sliding velocity vs. wear rate at 100 N Load (b) Load vs. wear rate at 1.257 (m/s) sliding velocity

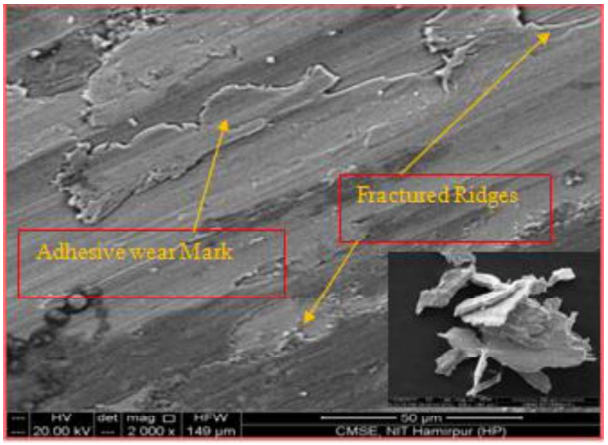

a.

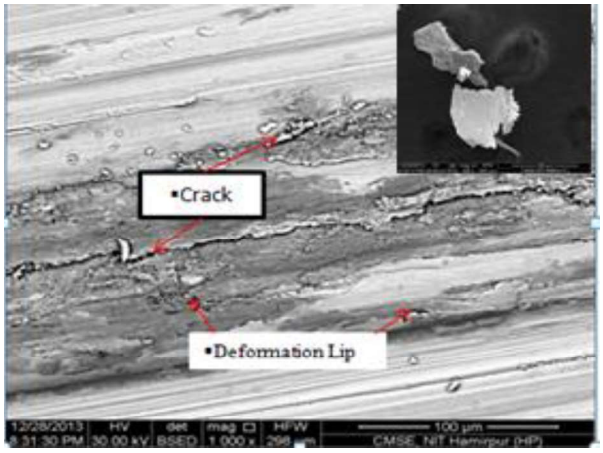

b.

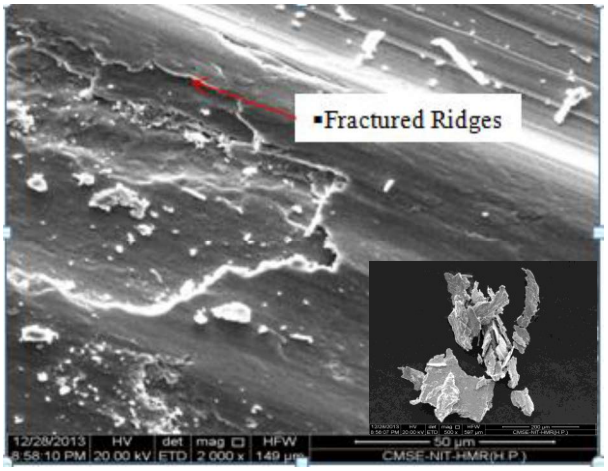

c.

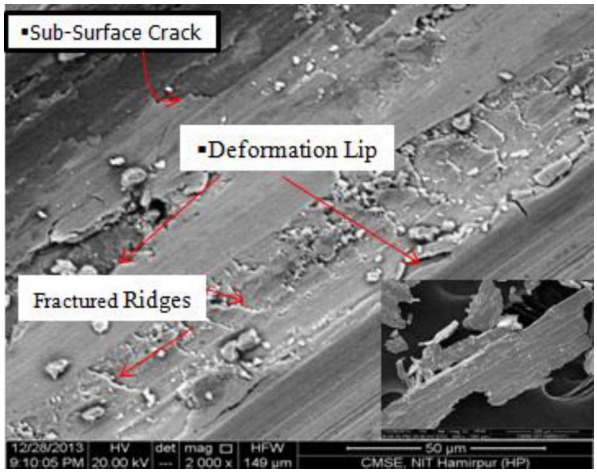

d.

Fig.7. Worn sample surfaces generated during wear experiment: load=140N and sliding velocity =1.885m/s for applied different treatment:(a)A3T, (b) C1-6, (c) C1-21 and (d) C1-36. Wear debris generated shown in the insets of respective sample FESEM micrograph

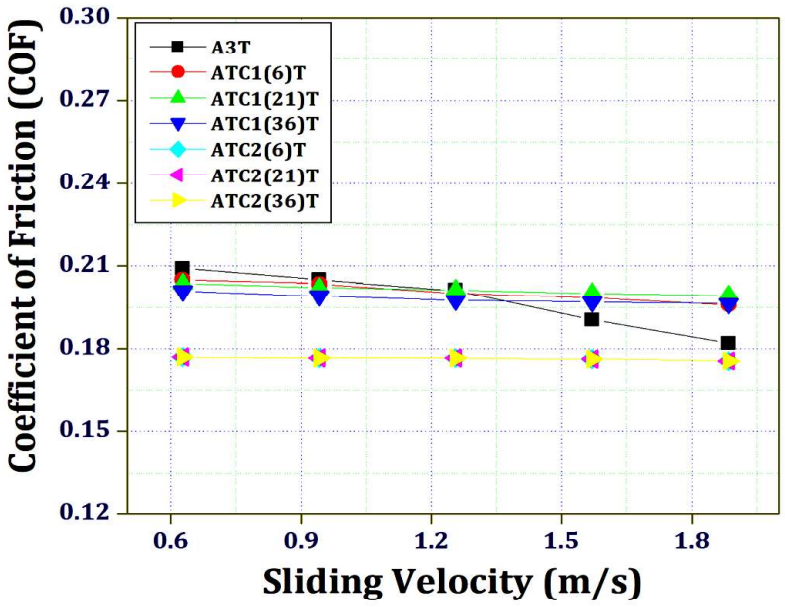

(a)

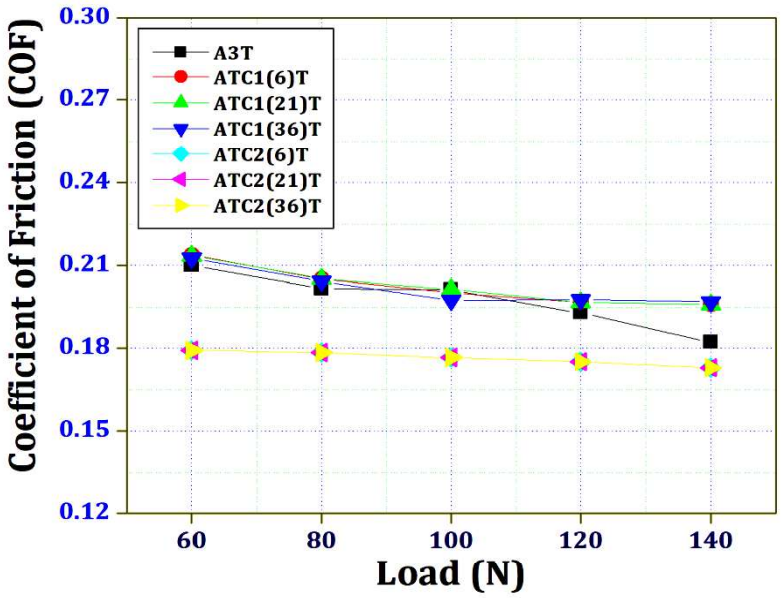

(b)

Fig. 8. Effect of process parameters on coefficient of friction (a) Sliding velocity vs. wear rate at 100 N Load (b) Load vs. wear rate at 1.257 (m/s) sliding velocity

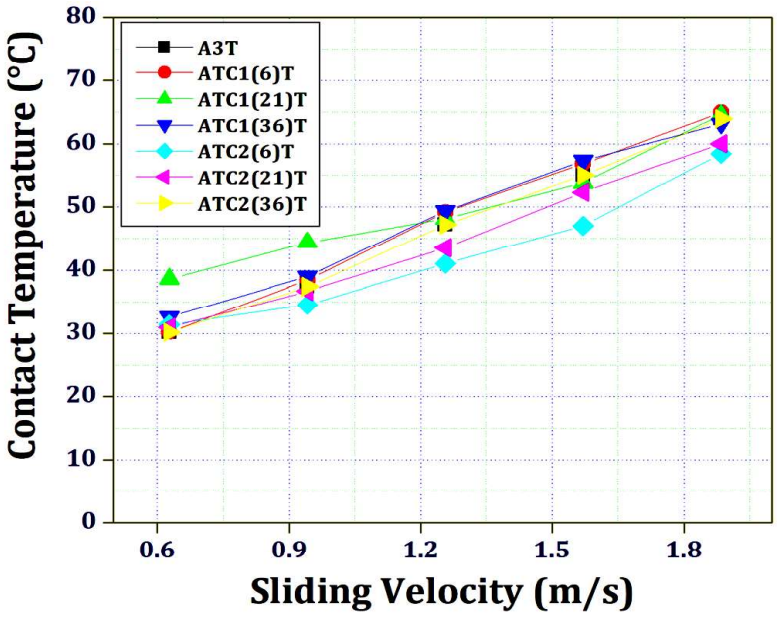

(a)

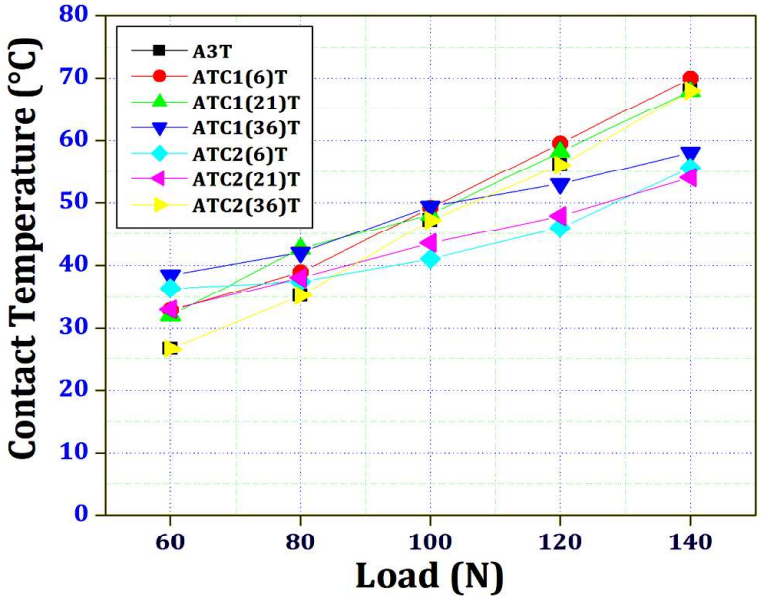

(b)

Fig. 9. Effect of process parameters on contact temperature (a) Sliding velocity vs. wear rate at 100 N Load (b) Load vs. wear rate 1.257 (m/s) sliding velocity

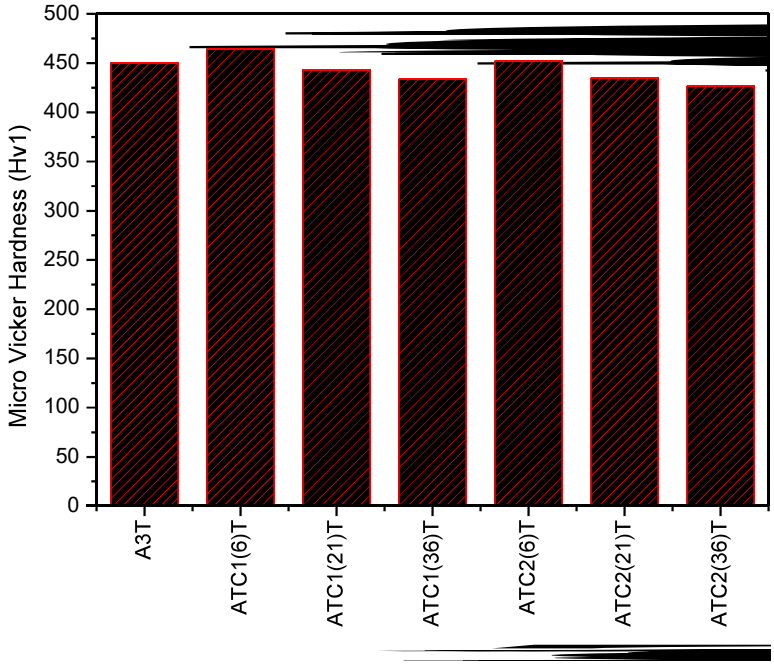

Fig. 10. Micro-hardness of varied treated samples.

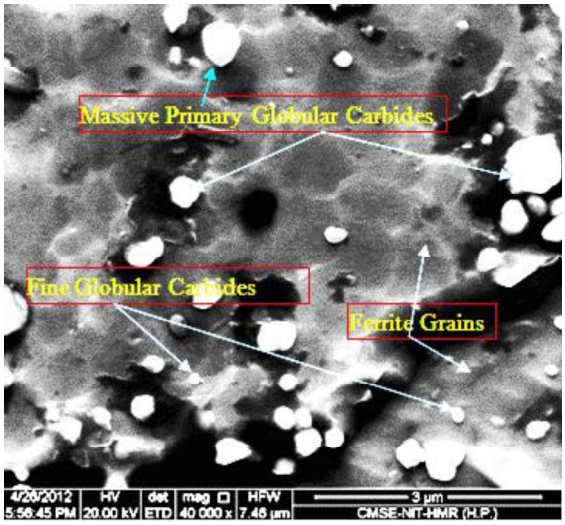
Massive Primary Globular Carbides
Fine Globular Carbides
Ferrite Grains
4/20/2012 5:56:45 PM HV 20.00 kV det ETD mag 40 000 x HFW 7.46 µm 3 µm CMSE-NIT-HMR (H.P.)

(a)

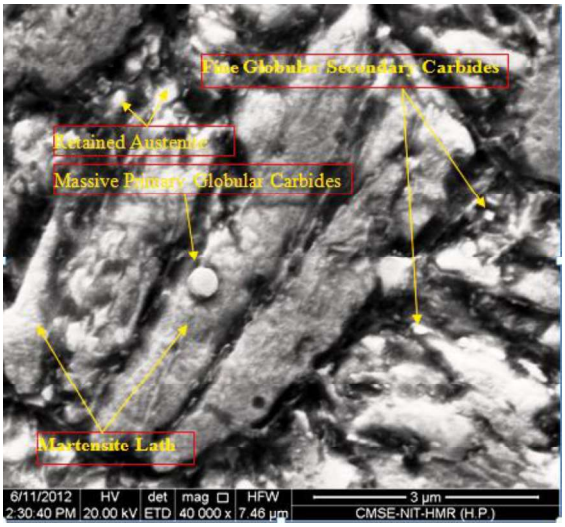
Fine Globular Secondary Carbides
Retained Austenite
Massive Primary Globular Carbides
Martensite Lath
6/11/2012 2:30:40 PM HV 20.00 kV det ETD mag 40 000 x HFW 7.46 µm 3 µm CMSE-NIT-HMR (H.P.)

(b)

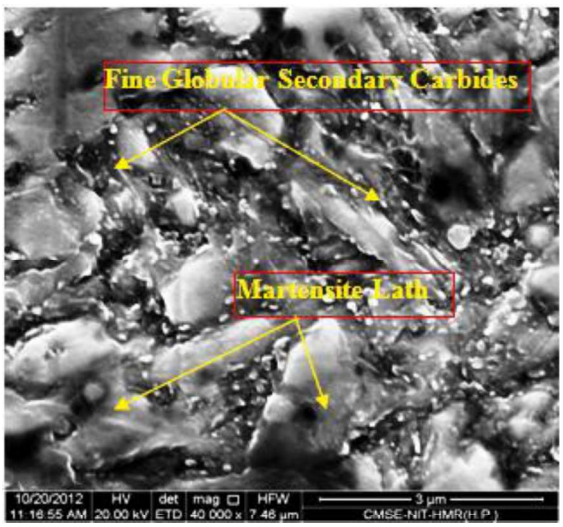
Fine Globular Secondary Carbides
Martensite Lath
10/20/2012 11:16:55 AM HV 20.00 kV det ETD mag 40 000 x HFW 7.46 µm 3 µm CMSE-NIT-HMR(H.P.)

(c)

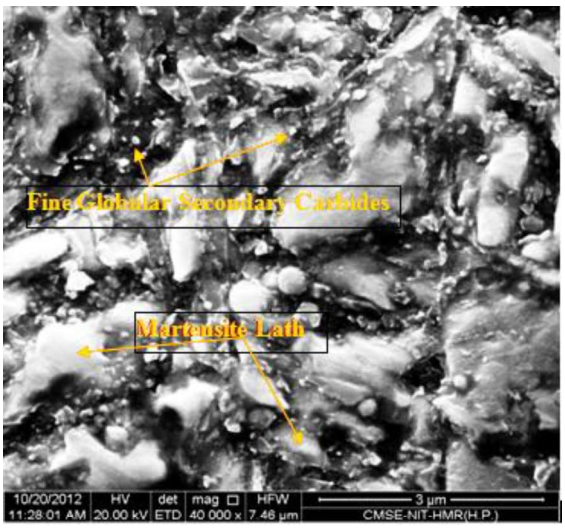
Fine Globular Secondary Carbides
Martensite Lath
10/20/2012 11:28:01 AM HV 20.00 kV det ETD mag 40 000 x HFW 7.46 µm 3 µm CMSE-NIT-HMR(H.P.)

(d)

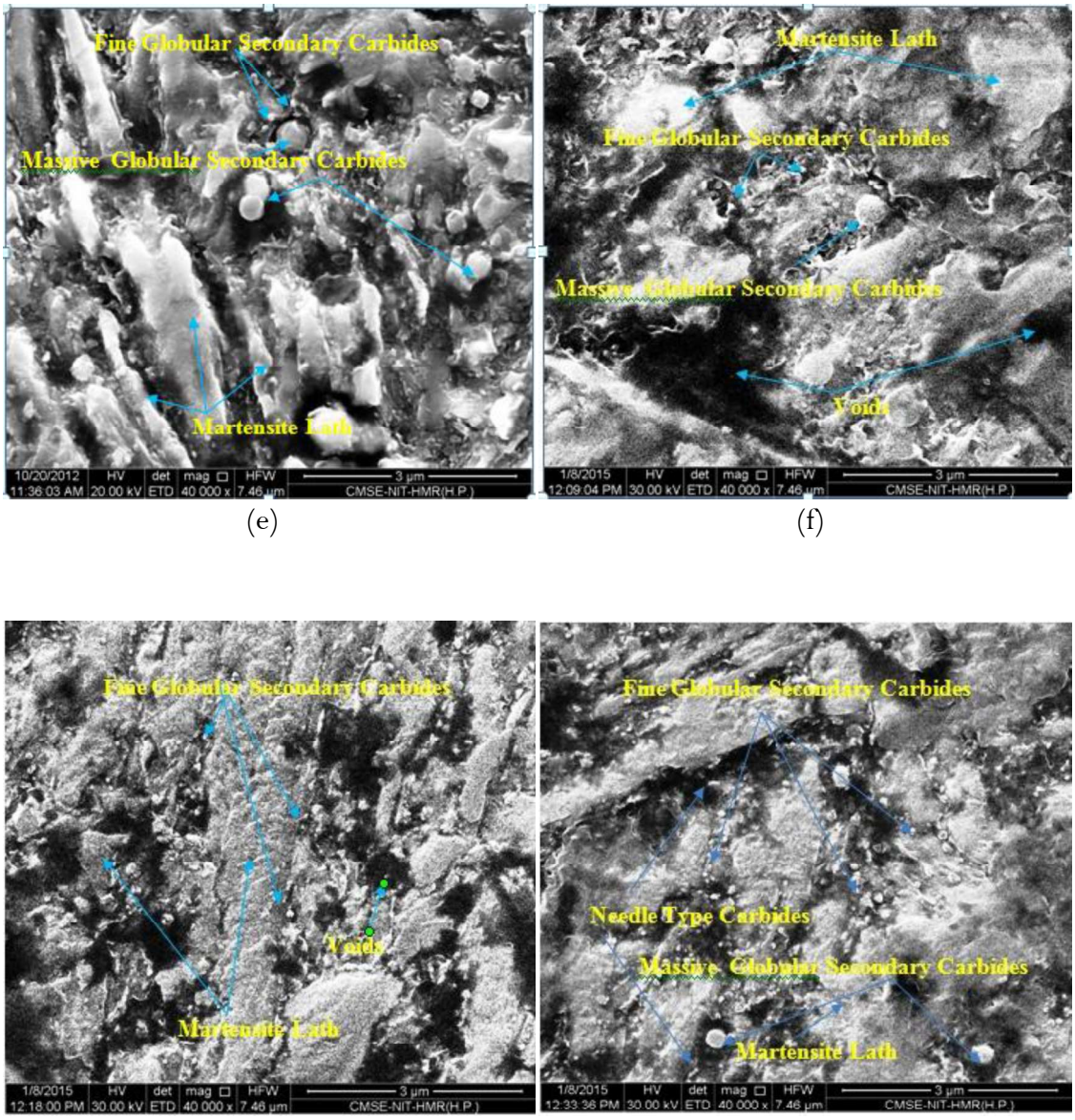

(e) (f)

(g) (h)

Fig. 11. FESEM micrographs AISI –H13 steel (a) in as received condition, and after different treatments: (b) A3T, (c) C1-6, (d) C1-21(e) C1-36, (f) C2-6, (g) C2-21, and (h) C2-36

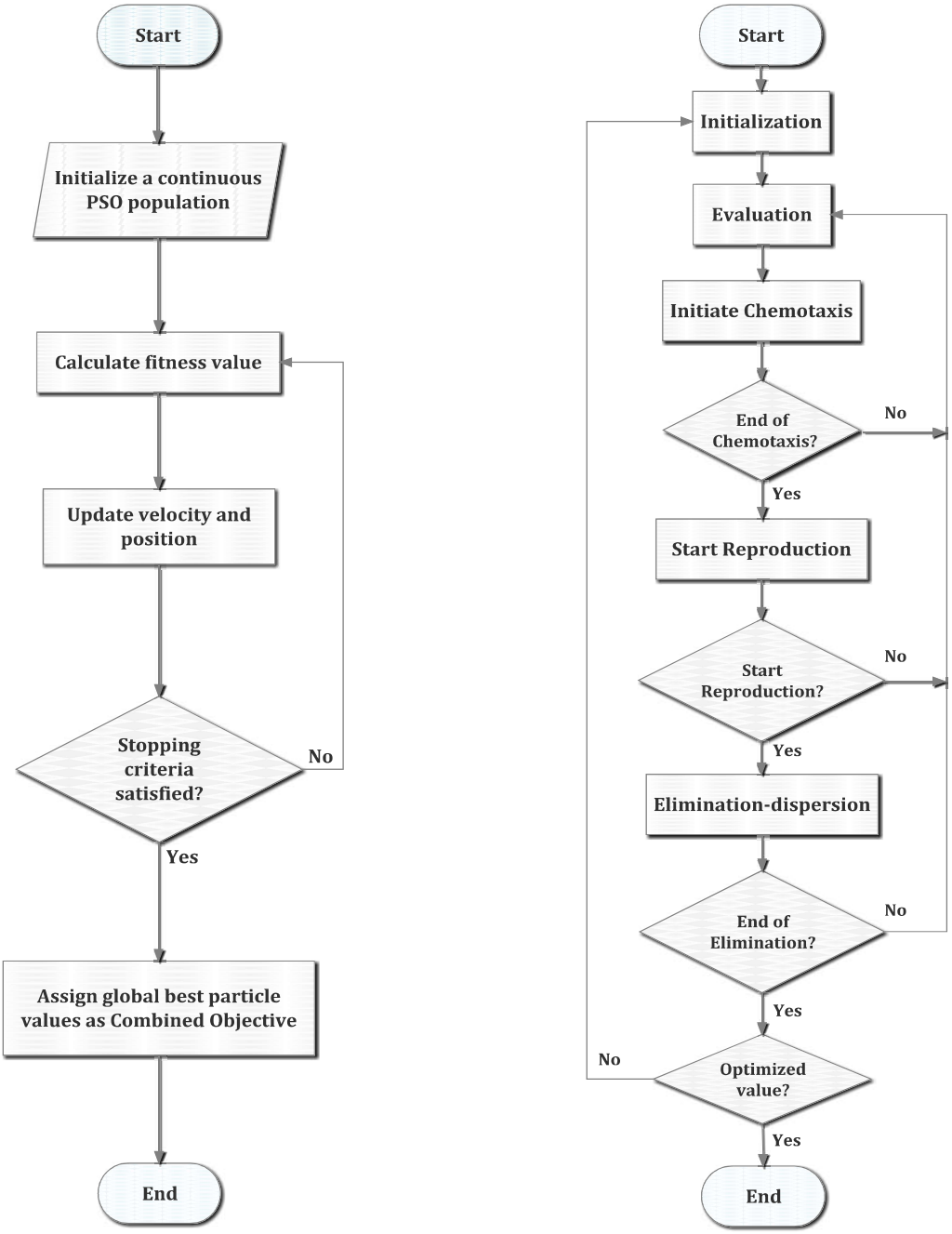

Fig.12. Flow Chart (a) PSO (b) BFO

Table(s)

Table 1 Heat treatment sequence followed

S .No.	Code	Type of treatment
1.	A3T	Three time tempered= 550°C, 570°C, 620°C respectively for 2 hours.
2.	C1-6	CT at −154°C for 6 hours followed by tempering at 620°C for 2 hours.
3.	C1-21	CT at −154°C for 21 hours followed by tempering at 620°C for 2 hours.
4.	C1-36	CT at −154°C for 36 hours followed by tempering at 620°C for 2 hours.
5.	C2-6	CT at −184°C for 6 hours followed by tempering at 620°C for 2 hours.
6.	C2-21	CT at −184°C for 6 hours followed by tempering at 620°C for 2 hours.
7.	C3-36	CT at −184°C for 6 hours followed by tempering at 620°C for 2 hours.

Table 2 Wear experiment variables and their different levels

Factor	Unit	Levels Values						
Treatment Type	-	A3T	C1-6	C1-21	C1-36	C2-6	C2-21	C2-36
Load	N	60	80	100	120	140	-	-
Sliding Speed	m/s	0.628	0.942	1.257	1.571	1.885	-	-

Table 3 Experimental responses for "W_R", "μ_o" and "T_M"

Wear rate (W_R) (gm/m)		Average co-efficient of friction (μ_o)		Maximum contact temperature (T_M) (°C)	
Minimum	Maximum	Minimum	Maximum	Minimum	Maximum
1.69×10^{-5}	1.48×10^{-4}	0.17	0.22	21.6	93.0

Table 4 Coefficient of determination values for "W_R", "μ_o" and "T_M"

Factors	Wear Rate (W_R)	Average co-efficient of friction(μ_o)	Maximum contact temperature (T_M)
R-Squared	0.9999	0.998	0.9901
Adj. R-Squared	0.9986	0.9973	0.9881
Pred. R-Squared	0.9981	0.9965	0.9844
Adeq. Precision	184.323	149.705	98.502
Model F-Value	8780.16	1547.72	481.2

Table 5 Optimization results for tribological parameters.

S. No.	Type of Treatment, (A)	Load (B), N	Sliding Velocity (C), m/s	Wear Rate (D), gm/m	Average Co-efficient of Friction, (E)	Contact Temperature (F), °C	Desirability
1	C2-21	60	0.687	1.73E-06	0.18	26.46	0.89
2	C2-21	60	0.682	1.73E-06	0.18	26.41	0.89
3	C2-21	60	0.696	1.73E-06	0.18	26.54	0.89
4	C2-21	60	0.703	1.74E-06	0.18	26.61	0.89
5	C2-21	60	0.661	1.74E-06	0.18	26.23	0.89

Table 6 Results of conformity tests for tribological parameters

Test No.	Process parameter			Response parameter (Predicted Value)			Response parameter (Experimental Value)			% Error		
	A	B (N)	C (m/s)	D (gm/m)	E	F (°C)	D gm/m	E	F (°C)	D gm/m	E	F (°C)
1	C2-21	60	0.687	1.73E-06	0.18	26.46	1.88E-06	0.18	24.5	8.67	2.08	7.41
2	C2-21	60	0.682	1.73E-06	0.18	26.41	1.83E-06	0.19	27.4	5.78	2.63	3.73
3	C2-21	60	0.696	1.73E-06	0.18	26.54	1.80E-06	0.19	24.9	4.04	3.19	6.18

Table 7 Parameters of PSO

Input parameters	Value of parameters
Number of variables	3 (dimension of search space)
Number of particles	46
Number of iterations	100
Inertia weight, W	0.7
Learning Rate	
C1max=C2max	1.7
C1min=C2min	0.5
C1=C2=Cmin+R*(Cmax-Cmin)	Where R = Current iterations/Total iterations
X_{min}	[1 60 0.628]
X_{max}	[6 140 1.885]

Table 8 Results of conformity tests for tribological parameters (PSO)

Test No.	Process parameter			Response parameter (Predicted Value by PSO)			Response parameter (Experimental Value)			% Error		
	A	B (N)	C (m/s)	D (gm/m)	E	F (°C)	D gm/m	E	F (°C)	D gm/m	E	F (°C)
1	C2-21	60	0.687	1.84E-06	0.17	24.5	1.88E-06	0.18	24.5	2.17	5.88	-0.37
2	C2-21	60	0.682	1.83E-06	0.17	27.1	1.83E-06	0.19	27.4	0	11.7	1.03
3	C2-21	60	0.696	1.84E-06	0.18	24.6	1.80E-06	0.19	24.9	-2.17	5.55	1.05

Table 9 Parameters of BFO

Input parameters	Value of parameters
p, dimension of search space	3
S, number of bacteria	60
N_c, number of chemotactic steps	100
N_{re}, number of reproduction steps	4
N_{ed}, number of elimination-dispersal events	5
N_s, maximum number of swim steps	4
P_{ed}, propability of elimination and dispersal	0.1
$C_{max,}$ maximum run length	0.2
C_{min}, minimum run length	0.01
R_U^p, Upper bound on search space	[1 60 0.628]
R_L^p, Lower bound on search space	[6 140 1.885]
$d_{attract}$= $d_{repellent}$, depth of attractant and repellent signals	0.1
$w_{attract}$, width of attractant signals	0.1
$w_{repellent}$, width of repellent signals	0.1

Table 10 Results of conformity tests for tribological parameters (BFO)

Test No.	Process parameter			Response parameter (Predicted Value by PSO)			Response parameter (Experimental Value)			% Error		
	A	B (N)	C (m/s)	D (gm/m)	E	F (°C)	D (gm/m)	E	F (°C)	D (gm/m)	E	F (°C)
1	C2-21	60	0.687	1.80E-06	0.17	23.8	1.88E-06	0.18	24.5	4.44	5.88	2.64
2	C2-21	60	0.682	1.81E-06	0.16	26.8	1.83E-06	0.19	27.4	1.10	18.75	1.97
3	C2-21T	60	0.696	1.80E-06	0.19	25.9	1.80E-06	0.19	24.9	0	0	3.97